Identification of novel peroxisome functions in yeast

Singh, Ritika

DOI:
10.33612/diss.99106402

CHAPTER 2

Identification of a novel peroxisomal peroxiredoxin in the yeast *Hansenula polymorpha*

Ritika Singh , Harshitha S. Kumar,
Rinse de Boer and Ida J. van der Klei

Molecular Cell Biology, Groningen Biomolecular Sciences and Biotechnology Institute, University of Groningen, the Netherlands

Abstract

2

Peroxisomes are ubiquitous cell organelles that play a central role in cellular lipid metabolism. Peroxisomes also possess enzymes to maintain redox balance and counteract oxidative stress. Recent studies resulted in the identification of several novel and often unexpected peroxisome functions, including non-metabolic roles. These novel functions are often related to stress and stress adaptations. The present study aims to extend the atlas of peroxisome functions by the identification of novel stress-related, yeast peroxisomal proteins. Through mass spectrometry analysis of peroxisomal fractions isolated from *Hansenula polymorpha* cells exposed to ethanol stress, we identified six putative peroxisomal peroxiredoxins. Two of them, named C8BNF3 and C8BNF4, contain a putative peroxisomal targeting signal 1. Peroxiredoxins are ubiquitous thiol-specific proteins that have multiple functions in stress protection, including defense against oxidative stress. The localization analysis using fusion proteins with green fluorescent protein and fluorescence microscopy indicated that C8BNF3 is a mitochondrial potein, whereas C8BNF4 partially localizes to peroxisomes in glucose-grown cells. The *c8bnf4* mutant displays no growth defect and shows no enhanced sensitivity to any of the stress conditions tested. Taken together, we have identified a novel peroxisomal peroxiredoxin in *H. polymorpha*, whose function remains to be established.

Introduction

Peroxisomes occur almost in all eukaryotic cells. These morphologically simple organelles consist of a single membrane which encloses a proteinaceous matrix. The number and metabolic functions of peroxisomes can strongly vary, depending on species, tissue, developmental stage and environmental conditions [1]. A characteristic feature of peroxisomes is the presence of enzymes of the β-oxidation pathway for the degradation of fatty acids. In addition, these organelles invariably contain H_2O_2 generating oxidases together with catalase. Examples of highly specialized functions include the metabolism of unusual carbon and nitrogen sources like methanol and D-amino acids in yeast or the biosynthesis of biotin or antibiotics in filamentous fungi [2].

In addition to the catabolic and biosynthetic processes peroxisomes are important in several non-metabolic functions, such as signaling, aging, antiviral innate immunity and defense against pathogens [3,4].

Peroxisomes greatly contribute to oxidative stress because of the presence of reactive oxygen species (ROS) producing enzymes[5]. The peroxisomal redox balance does not only affect peroxisome related processes such as matrix protein import [6] and organelle proliferation [7], but also can affect molecules and processes at other subcellular locations. For instance reactive oxygen species (ROS) released from peroxisomes can have a toxic effect on DNA, proteins or lipids, but can also cause dysregulation of ROS signaling pathways [8]. Here we aimed to identify novel (oxidative) stress related proteins in peroxisomes of the yeast *Hansenula polymorpha*.

To this purpose we performed organelle proteomics using peroxisomes isolated form cells that were exposed to stress. This approach resulted in the identification of a novel peroxiredoxin that is partially localized to peroxisomes.

Results

Exploration of suitable stress conditions

In order to identify novel, stress-related peroxisomal proteins by organelle proteomics, we first needed to find suitable stress conditions. To this purpose, we used three reporter strains in which the gene encoding super folder Green Fluorescent Protein (sfGFP) is expressed under control of a promoter of a gene encoding a peroxisomal protein that is likely induced by various stress conditions (i.e. catalase, *CAT*[9] , the peroxisomal Lon protease, *PLN*[10] and the peroxisomal peroxiredoxin *PMP20* [11]). Cells were grown in batch cultures on media containing glycerol, conditions that do not repress established *H. polymorpha* peroxisomal proteins. Upon exposure of the cells to various chemical or temperature stress conditions, the sfGFP levels were monitored by flow cytometry. As shown in Fig. 1A, the highest induction of the catalase promoter (P_{CAT}) was obtained upon exposure of cells to 5 mM H_2O_2, or 6 % ethanol. The promoters P_{PLN} or P_{PMP20} were not induced by any of the stress conditions tested. Further analysis using different hydrogen peroxide and ethanol concentrations indicated that induction of P_{CAT} was also

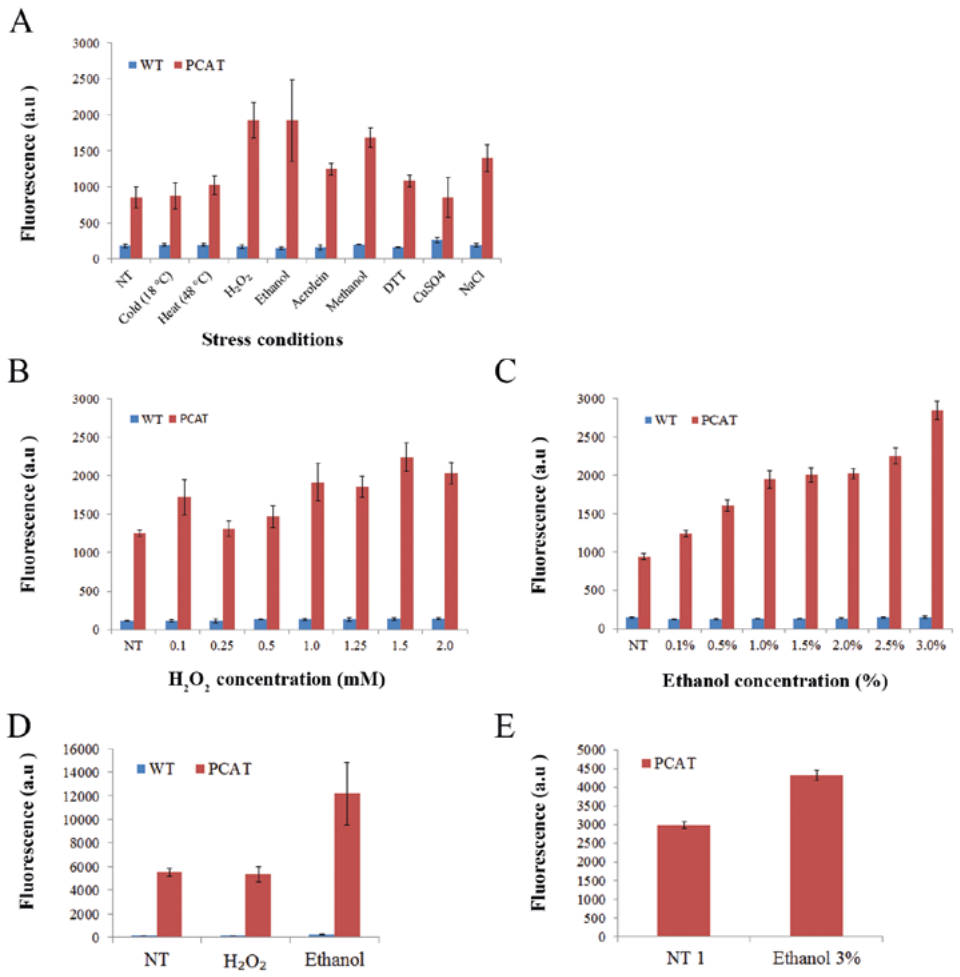

Figure 1. Ethanol stress induces the catalase promoter. (A) Fluorescence measured by FACS in WT cells (background) and cells of WT strains containing P_{CAT} sfGFP, P_{PMP20} sfGFP or P_{PLN} sfGFP, grown for 16 h in medium containing 0.2 % glycerol exposed to the indicated stressors for 1 hour. The concentrations used were 5 mM H_2O_2, 6% (v/v) ethanol, 4.3 % (v/v) methanol, 0.7 M NaCl, 0.1 mM acrolein, 30 mM DTT or 2 mM $CuSO_4$: Data represents mean fluorescence. NT – Not treated. (B) Analysis of effect of different H_2O_2 and (C) ethanol concentrations to induce P_{CAT} in glycerol-grown cells. P_{CAT} activity was significantly higher than the NT when 1 mM, 1.25 mM, 1.5 mM and 2 mM H_2O_2 was used. (D) Effect of H_2O_2 (1.5 mM) and ethanol (3%) on cells grown in methanol containing batch cultures. (E) Effect of 3% ethanol on methanol-limited chemostat grown cells. Data represents mean ± SD, n=2.

obtained using lower concentrations of hydrogen peroxide or ethanol (Fig 1B,1C). Based on the outcome of this experiment we decided to use 1.5 mM H_2O_2 and 3 % ethanol for all further experiments.

Next, we tested the activity of P_{CAT} in cells grown in batch cultures containing methanol, a growth condition that induces peroxisome proliferation. At these conditions sfGFP expression

from P_{CAT} also increased after treatment of cells with ethanol, but no effect was observed upon exposure to H_2O_2 (Fig 1 D).

Peroxisome proteomics of stressed and unstressed cells

Based on the above results we decided to perform organelle proteomics using cells exposed to 3% ethanol. Peroxisomes were isolated from methanol-limited chemostat cultures, growth conditions that lead to massive peroxisome proliferation facilitating the isolation of the organelles for proteomic analysis. As shown in Fig. 1E, P_{CAT} activity also increased upon exposure of chemostat grown cells to ethanol stress. Organellar pellets derived from ethanol stressed cells as well as untreated controls were subjected to sucrose density gradient centrifugation. Peroxisomal marker proteins were enriched in fractions of high density, as expected. Based on enzyme measurements of the mitochondrial marker enzyme cytochrome c-oxidase, we concluded that relatively pure peroxisome fractions were obtained from both unstressed (Fig. 2A) and stressed cells (Fig. 2B).

Mass Spectrometry (MS) resulted in the identification of 100 different proteins in the control sample and 59 proteins in the peroxisomal fraction isolated from the ethanol-stressed cells (Table S1). As expected, all known major *H. polymorpha* peroxisomal proteins were identified by MS in both fractions. Comparison of the data revealed large overlap between both lists. Analysis of the *Saccharomyces cerevisiae* genome database (SGD; https://www.yeastgenome.org/) revealed that from the putative *S. cerevisiae* homologues of the 100 identified *H. polymorpha* proteins 23 are annotated as being peroxisomal (Fig. 2C).

The identification of novel putative peroxisomal peroxiredoxins

In organellar fractions isolated from both stressed and unstressed cells the well established peroxisomal peroxiredoxin Pmp20 was identified, together with 6 novel, putative peroxiredoxins. Multiple alignments of the amino acid sequences of these peroxiredoxins showed that they shared >25% sequence identity (Fig. 3). Furthermore, HHpred [12] and InterProScan [13] suggests that all 7 proteins have a thioredoxin domain and belong to the AhpC/TSA family, which contains proteins related to alkyl hydroperoxide reductase (AhpC) and thiol specific antioxidant enzyme (TSA). Also, sequence analysis revealed that three of the proteins, including Pmp20, contain a putative Peroxisomal Targeting Signal 1 (PTS1) at their extreme C-terminus. Because Pmp20 is already studied in detail, the other two peroxiredoxins with a predicted PTS1 were further analyzed. These peroxiredoxins are designated C8BNF3 and C8BNF4 (based on the UniProt database), respectively.

C8BNF3 is localized to mitochondria

We first performed fluorescence microscopy (FM) using strains producing C8BNF3 containing green fluorescent protein (GFP) either at the N- or C-terminus, in order to validate its subcellular localization (Fig. 4A). GFP-C8BNF3 was produced under control of amine oxidase promoter (P_{AMO}), whereas C8BNF3-GFP was produced under control of the endogenous promoter.

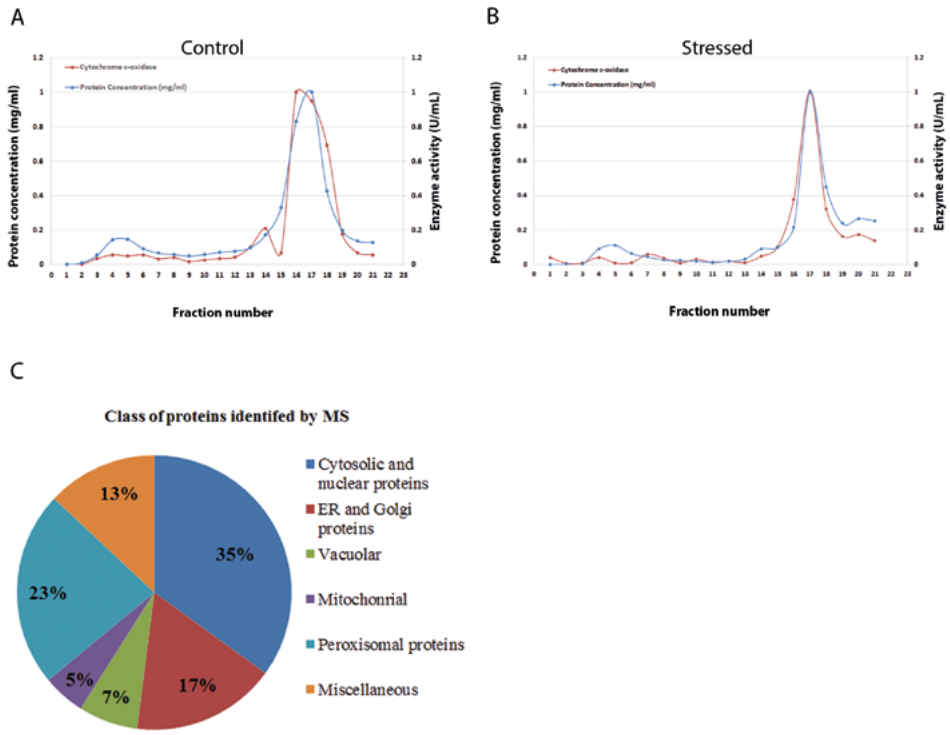

Figure 2. Mass spectrometry analysis of peroxisomal fractions. Peroxisome fractions isolated from control (without stress) **(A)** and ethanol stressed cells **(B)** using sucrose density gradient fractionation of organellar pellets. Cells were grown in a carbon limited chemostat on a mixture of 0.25% Glucose + 0.25 % methanol at a dilution rate of 0.1 h^{-1}. For the stressed sample, cells were exposed to 3% ethanol for one hour. The fractions of the sucrose gradient were analyzed for the presence of cytochrome c-oxidase activity and protein concentrations. Graph representing protein concentration and cytochrome c-oxidase activities. Activity expressed as units per mg of protein. Protein concentrations were measured using Bradford assay. A pie chart summarizing subcellular distribution of the putative *S. cerevisiae* homologues of the 100 *H. polymorpha* proteins identified by MS analysis that were detected in the peroxisomal peak fraction of the control sample **(C)**.

In glucose/methylamine-grown cells GFP-C8BNF3 fluorescence was present in spots, as well as in structures, which may represent the ER and nuclear envelope. Green fluorescence in the cytosol was very low. The spots represent peroxisomes, as they co-localized with the peroxisomal matrix marker DsRed-SKL (Fig. 4Ba). In methanol/methylamine grown cells, GFP-C8BNF3 fluorescence was less evident at the cell periphery. Again, the protein localized to peroxisomes, displaying clusters of ring structures, typical for peroxisomal membrane proteins, together with low cytosolic fluorescence (Fig. 4Bb).

The fluorescence pattern of the cells producing the C-terminally GFP tagged protein was very different and suggest a mitochondrial localization both in cells grown on glucose/ammonium or methanol/ammonium containing medium (Fig. 4C). Because a C-terminal GFP

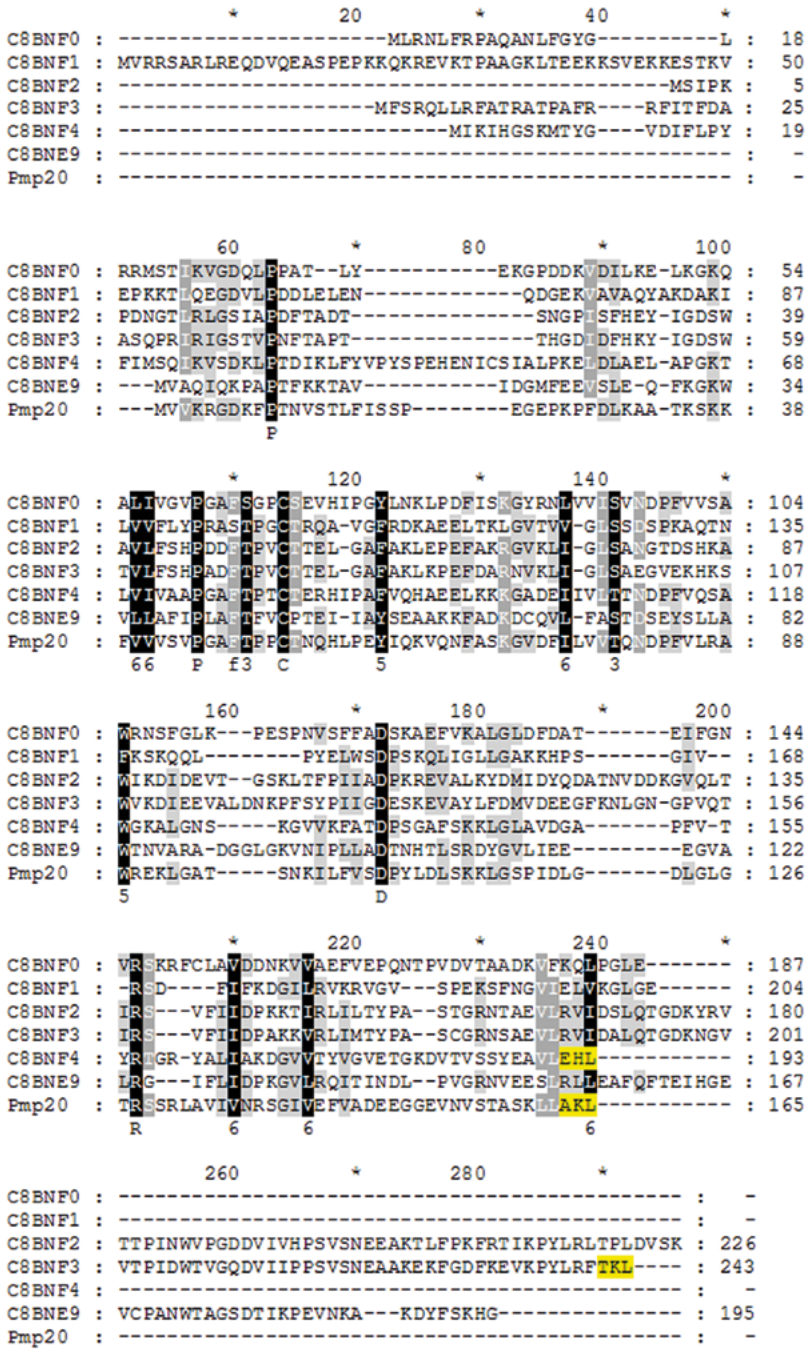

Figure 3. Sequence alignment of 7 identified *H. polymorpha* peroxiredoxins. All the identified peroxiredoxins sequences were aligned using ClustalW and visualized with Genedoc. Black shading indicates identity. Similarity is indicated as white letters that are shaded dark grey and light grey. Putative PTS1 sequences shaded in yellow.

obstructs the PTS1 and an N-terminal GFP the N-terminal mitochondrial pre-sequence, we generated antibodies against C8BNF3 in order to localize the untagged protein by immuno-electron microscopy. In cells extracts of WT cells, the antiserum specifically recognized

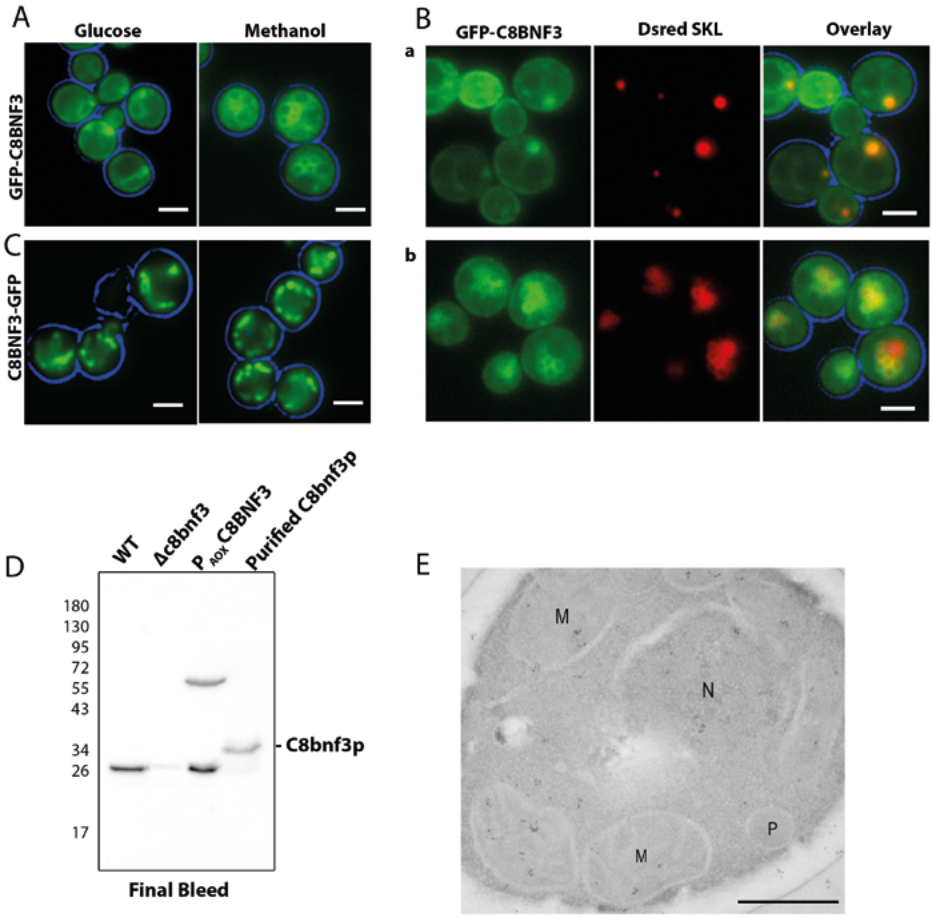

Figure 4. C8BNF3 localises to mitochondria in *H. polymorpha*. **(A)** FM images of WT cells expressing GFP-C8BNF3 under control of P_{AMO} grown on glucose/methylamine and methanol/methylamine. Scale bars represent 2µm. (B) FM images of WT cells expressing C8BNF3 tagged with GFP at the N-terminus and producing DsRed-SKL grown on glucose (a) or methanol (b). Scale bars represent 2µm **(C)**. FM analysis of cells producing C8BNF3 containing GFP at the C-terminus grown on glucose/ammonium sulphate and methanol/ammonium sulphate. (D) Western blot prepared from crude extracts of glucose grown WT, Δ*c8bnf3*, WT expressing P_{AOX}-C8BNF3-GFP, and purified His_6-tagged C8BNF3 protein, showing the specificity of the polyclonal anti-C8BNF3 antiserum. (E) Immuno-Electron microscopy image showing WT cells grown on glucose. C8BNF3 was labelled with antibodies against C8BNF3 and detected with goat anti-rabbit antibodies conjugated to 6-nm gold particles. M-Mitochondria, N-Nucleus, V-Vacuole. Scale bar represents 200nm.

a protein band of 27 kD, which is the expected molecular mass based on its amino acid composition. This band is absent in extracts prepared from cells of a C8BNF3 deletion strain (*Δc8bnf3*; Fig. 4D). As expected a second and larger band (approx. 55 kDa) was observed upon introduction of a C8BNF3-GFP fusion protein in WT cells. In the Western blot of the purified protein, a band of approx. 34 kDa was observed. The increased size is due to the presence of the His_6 tag in the purified protein.

Immuno-labelling experiments of WT cells grown on glucose containing medium using anti-C8BNF3 antibodies resulted in labelling of mitochondrial profiles, supporting the conclusion that the untagged protein is most likely mitochondrial (Fig. 4E).

C8BNF4 is partially localized to peroxisomes

To investigate the localization of C8BNF4 a strain was constructed that contains a gene encoding C8BNF4 containing GFP at the N-terminus (GFP-C8BNF4) under control of the P_{AMO}. In glucose/methylamine-grown cells, the N-terminal fusion protein appeared mostly cytosolic, but in many cells a spot was present as well (Fig. 5A). These spots represent peroxisomes because they co-localize with DsRed-SKL (Fig. 5B). The GFP signal appeared predominantly in the cytosol in methanol/methylamine grown cells, but occasionally small spots were detected (Fig. 5A,B). Based on these observations we conclude that at these growth conditions C8BNF4 does not accumulate in the relatively large peroxisomes that are predominantly present in methanol-grown cells. The C-terminally tagged C8BNF4 (C8BNF4-GFP) produced under control of its own promoter was mainly cytosolic when cells were either grown on glucose or methanol (Fig 5C). This result suggests that the PTS1 of C8BNF4 is a genuine PTS.

C8BNF4 is not required for growth on glucose or methanol

To analyse the function of C8BNF4 a deletion strain was constructed (*Δc8bnf4*). Growth experiments revealed that *Δc8bnf4* cells grow normal on glucose and methanol containing media (Fig 6A). The presence of a thioredoxin-like domain in C8BNF4 suggests that this protein might function as antioxidant enzyme. In order to test the sensitivity of the deletion mutant to oxidative stress, cells of the deletion strain were grown to the stationary phase on glucose and spotted onto plates containing- H_2O_2, the free radicals producing compounds tertiary butyl hydroperoxide (BHP), the catalase inhibitor amino triazole- AT, the reducing agent dithiothreitol (DTT), NaCl or ethanol as stressors. Growth was compared to WT controls, as well as *pmp20* cells and cells of a *Δc8bnf4 Δpmp20* double deletion strain. The results revealed that these stress conditions did not affect growth of any of the strains used (data not shown). We finally examined C8BNF4 protein levels upon exposure to the stress condition used for peroxisome proteomics experiment. Glucose grown cells were exposed to ethanol stress for 2 hours. Western blot analysis revealed that the levels of C8BNF4 do not significantly change when the cells were exposed to ethanol stress (Fig. 6B).

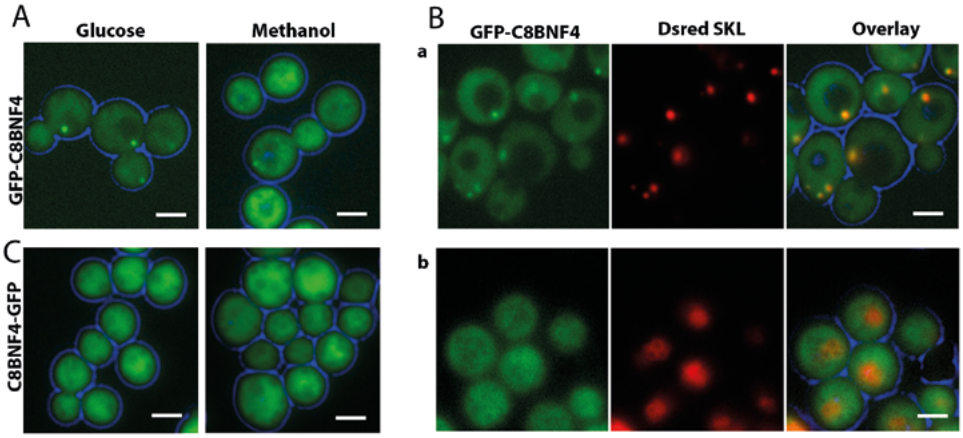

Figure 5. C8BNF4 localises to peroxisomes in cells grown on glucose, but not in methanol-grown cells. FM images of WT cells expressing GFP-C8BNF4 under control of the P_{AMO}. (A) without peroxisomal marker and (B) with the peroxisomal marker DsRed-SKL grown on glucose/methylamine (Ba) or methanol/methylaine (Bb). Scale bars represent 2µm. (C) Fluorescence microscopy analysis of cells producing C8BNF3 containing GFP at the C-terminus grown on glucose/ammonium sulphate and methanol/ammonium sulphate.

Discussion

Using organelle proteomics of *H. polymorpha* peroxisomes, we identified a novel PTS1 containing peroxiredoxin, C8BNF4, which localizes to peroxisomes in glucose-grown cells, but does not accumulate in peroxisomes in methanol-grown cells. The level of this protein was not significantly enhanced in cells exposed to compounds that are known to cause oxidative stress such as TBA, AT and hydrogen peroxide.

Analysis of the activity of promotors encoding stress related peroxisomal proteins, indicated that the *CAT* promotor showed increased activity upon exposure of the cells to ethanol at all growth conditions tested. Therefore we decided to use ethanol exposure a stress condition for the identification of novel stress inducible peroxisomal proteins by organelle proteomics.

While ethanol is can be produced by several yeast species, , it also can be harmfull causing alterations in mitochondrial membrane integrity, reduction in respiratory rates and ATP levels and production of ROS and acetaldehyde, which ultimately results into DNA damage, lipid peroxidation and oxidative stress [14]. *H. polymorpha* has also been reported to ferment sugars to ethanol but the effect of high concentrations of ethanol is not yet explored [15].

Exposure of glycerol- or methanol-grown *H. polymorpha* cells to externally added ethanol is most likely also toxic because the alcohol oxidase enzyme present in these cells will oxidize ethanol into H_2O_2 and acetaldehyde [90].

We were able to obtain peroxisomal fractions from both unstressed and stressed cells, which is supported by the fact that all known *H. polymorpha* peroxisomal proteins such as alcohol

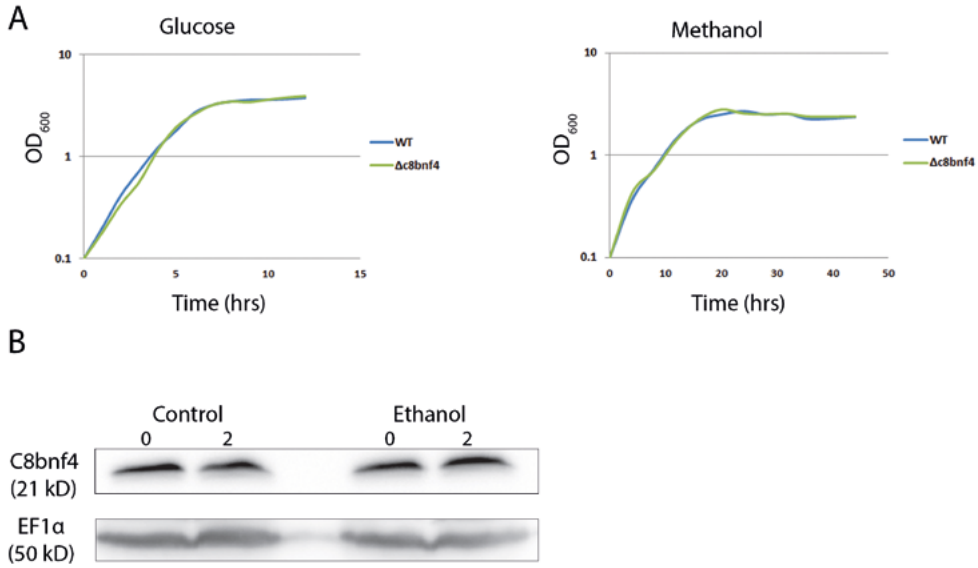

Figure 6. *c8bnf4* cells show normal growth on methanol as well as glucose containing medium. Growth curve of *c8bnf4* and WT control cells in glucose medium and methanol containing medium **(A)**. C8BNF4 protein levels upon exposure of WT cells to 3% ethanol. Cells were grown on glucose containing media. Representative western blots showing the protein levels of C8BNF4 upon exposure to ethanol for 2 hours. Blots were probed with antibodies against C8BNF4. Elongation factor 1 α (EF1α) was used as loading control **(B)**.

oxidase, dihydroxyacetone synthase, catalase, Pmp20 and several peroxins were identified. Proteomic analysis resulted in the identification of similar proteins in organelles isolated from stressed and unstressed cells. Furthermore, the list of proteins present in the organellar fraction of the organelles obtained from the stressed cells was shorter when compared to the list of the unstressed cells. As we did not perform quantitative proteomics, it is difficult to draw any conclusions from this observations.

Several putative peroxiredoxins were identified in both fractions. The presence of multiple peroxiredoxins in one species is common. *S. cerevisae* contains 5 peroxiredoxins and at least 6 peroxiredoxins occur in mammals. Peroxiredoxins are important for antioxidant defense and their absence can lead to ROS/reactive nitrogen species (RNS) accumulation. Surprisingly, we have identified 7 *H. polymorpha* peroxiredoxins in both peroxisome fractions including the previously studied peroxisomal protein Pmp20. In addition to Pmp20, two yet uncharacterized peroxiredoxins (C8BNF3 and C8BNF4) appeared to have a PTS1 targeting signal**.**

Sequence analysis revealed that C8BNF3 exhibited significant sequence similarities with the *S. cerevisiae* thiol peroxidase Prx1 [16] and human Prx6. Using immunoblot analysis of subcellular fractions ScPrx1 has been reported to be localized to mitochondria [17], whereas the human Prx6 was localized to the cytosol [18–20]. Like ScPrx1, *H. polymorpha* C8BNF3 has

a mitochondrial targeting sequence predicted by Mitoprot [21]. Indeed, we observed that upon tagging C8BNF3 with GFP at the C-terminus, the protein localizes to mitochondria. Unlike the putative *S. cerevisiae* and *H. sapiens* homologues, C8BNF3 also has a putative PTS1 targeting signal (TKL). This led us to speculate that C8BNF3 might show a dual localization to mitochondria and peroxisomes. Our immunolabelling studies suggests that untagged C8BNF3 predominantly localizes to mitochondria (Fig 4), but these experiments do not exclude that a minor portion could be peroxisomal or cytosolic.

C8BNF4 exhibits significant sequence similarities with *S. cerevisiae* Ahp1 [16] and human Prx5. C8BNF4 has a PTS1 (EHL), like ScAhp1 and HsPrx5 (AHL and SQL respectively). HsPrx5 also possess a mitochondrial targeting sequence and has been reported to be localized to mitochondria, peroxisomes, and the cytosol [22,23]. It is proposed that HsPrx5 preferentially localizes to mitochondria. The mechanism responsible for the subcellular localization of Prx5 to several cellular compartments is still not clear. On the other hand, even though ScAhp1 has a PTS1 signal, the functionality of this signal has not yet been proven. Ahp1 localization to the cytosol has been shown using fluorescence microscopy and immunoblot analysis of cytosolic and peroxisomal fractions [16]. Unlike *S. cerevisae* Ahp1, our localization studies of C8BNF4 indicate that it exists in peroxisomes when cells are grown on glucose and predominantly in the cytosol when grown on methanol. However, we cannot rule out the possibility that overproduction of the N-terminal GFP fusion of C8BNF4, may affect the localization. *S. cerevisae* has been reported to contain 5 peroxiredoxins. Several paralogs exist and so far, none of the *S. cerevisiae* peroxiredoxins have been reported to be localized to peroxisomes. The cytosolic localization of C8BNF4 in methanol grown *H. polymorpha* cells could be due to inefficient import into peroxisomes or functional redundancy.

Apart from catalase, detoxification of peroxisomal ROS also involves peroxiredoxins and glutathione peroxidases. Mammalian peroxisomes contain two antioxidant enzymes, superoxide dismutase [91] and glutathione peroxidase Gpx [24]. Methylotrophic yeast species contain the peroxiosmal peroxiredoxin Pmp20 [11] whereas *S. cerevisae* contains glutathione peroxidases Gpx1 [7]. HpPmp20 is induced on methanol. Cells lacking Pmp20 show a severe growth defect on methanol together with ROS accumulation. No growth defect was observed for the C8BNF4 deletion mutant. Also, the deletion mutant was not sensitive to any of the stressors tested. Our findings corroborate with the previous reports indicating that yeast mutants lacking multiple peroxiredoxins were more susceptible to ROS/RNS stress when compared to a single deletion mutant [25].

In summary, we have characterized two novel *H. polymorpha* peroxiredoxins, which have functional PTS1 targeting signals. The identified peroxisomal peroxiredoxin is not essential for growth of cells at peroxisome reducing (glucose) or inducing (methanol) conditions. Also, it is not essential for the tolerance of cells to oxidative stress. A possible explanation could be that the presence of many other peroxiredoxins might be compensating, enabling the mutant to survive under stress conditions.

Materials and methods

Strains and growth conditions. All *H. polymorpha* strains used in this study are derivatives of the NCYC495 WT strain (Table 1). Cells were grown in batch cultures at 37°C on mineral media [26] supplemented with 0.25% glucose, 0.2% glycerol or 0.5% methanol, as carbon source and 0.25 % ammonium sulphate or 0.25% methylamine as nitrogen source. When required leucine was added to a final concentration of 30 μg/ml. For growth on plates, YPD (1 % yeast extract, 1 % peptone and 1 % glucose) medium was supplemented with 2 % agar. Transformants were selected using 100 μg/ml zeocin (Invitrogen), 100 μg/ml nourseothricin (Werner Bioagents) or 200 μg/ml hygromycin (Invitrogen). *Escherichia coli* DH5a was used for cloning. Cells were grown at 37°C in Luria Bertani (LB) medium (1% bacto tryptone, 0.5% yeast extract and 0.5% NaCl) supplemented with ampicillin (100 μg/ml) or kanamycin (50 μg/ml). For growth on agar plates, 2% agar was added to LB medium. Optical densities of cultures were measured at 600nm.

For peroxisome isolation, cells were grown in a chemostat using mineral medium containing 0.25% glucose and 0.25% methanol at a dilution rate of 0.1 h^{-1}.

In the stress experiments, cells were exposed to tertiary butyl hydroperoxide (BHP), amino triazole (AT), dithiothreitol (DTT), NaCl, ethanol, H_2O_2, methanol, acrolein, or $CuSO_4$ [27–30]. For temperature stress, cells were incubated at 18°C or 48 °C for 1 hour

Cloning and strain construction

The plasmids and primers used in this study are listed in Table 2 and Table 3. *H. polymorpha* was transformed as describes before [31]. All integrations were checked by colony PCR. Gene deletions were also confirmed by southern blotting.

Table 1. *Hansenula polymorpha* strains used in this study.

Strain	Description	Reference
WT	NCYC 495 *leu1.1*	24
WT DsRedSKL	NCYC 495 *leu1.1*	23
PMP47_GFP	NCYC 495 *YKU80 le1.1 Nat*$^+$	25
GFP_C8BNF3 DsRed SKL	NCYC 495 *Nat*$^+$ *leu*$^-$	This study
GFP_C8BNF4 DsRed SKL	NCYC 495 *Nat*$^+$ *leu*$^-$	This study
GFP_C8BNF3	NCYC 495 *leu*$^-$ *Nat*$^+$	This study
GFP_C8BNF4	NCYC 495 *leu*$^-$ *Nat*$^+$	This study
C8BNF3_GFP	NCYC 495 *leu*$^-$ *Nat*$^+$	This study
C8BNF4_GFP	NCYC 495 *leu*$^-$ *Nat*$^+$	This study
Δc8bnf3 PMP47_GFP	NCYC 495 *KU80 leu*$^-$ *Nat*$^+$ *Zeo*$^+$	This study
Δc8bnf4 PMP47_GFP	NCYC 495 *KU80 leu*$^-$ *Nat*$^+$ *Hyg*$^+$	This study
Δpmp20	*PMP20*::*URA3*, *leu*1.1	11
Δc8bnf4 Δpmp20	NCYC 495 *KU80 leu*$^-$ *Nat*$^+$ *Zeo*$^+$ *Hyg*$^+$	This study

Table 2. List of plasmids used in this study.

Plasmids	Description	Reference
pHIPZ_P_{PMP20}–sfGFP	pHIPZ plasmid containing sfGFP under control of *PMP20* promoter, zeocine resitance cassette, amp^R	This study
pHIPZ_P_{CAT}–sfGFP	pHIPZ plasmid containing sfGFP under control of *CAT* promoter, zeocine resistance cassette, amp^R	This study
pDONR 221	Standard Gateway vector	19
pDEST R4R3	Standard Gateway vector	19
pENTR P_{AMO} GFP	pDONR-P4-P1R containing $P_{AOX/}$ kan^R	23
pENTR23_T_{AMO}	pDONR-23 containing *AMO* terminator/kan^R	23
pENTR C8BNF3	pENTR-221 containing *C8BNF3/* kan^R	This study
pENTR C8BNF4	pENTR-221 containing *C8BNF4/* kan^R	This study
pDEST-R4-R3	Standard Gateway vector	19
pDEST P_{AMO} GFP C8BNF3 T_{AMO}	pDEST-R4-R3-NAT containing GFP_C8BNF3 under control of amine oxidase promoter/amp^R	This study
pDEST P_{AMO} GFP C8BNF4 T_{AMO}	pDEST-R4-R3-NAT containing GFP_C8BNF4 under control of amine oxidase promoter/amp^R	This study
pHIPZ mGFP Fusinator	pHIPZ containing mGFP and *AMO* terminator/amp^R	27
pMaM17	Plasmid containing mcherry-sfGFP	12
pSEM04	pHIPH5 containing *PEX3* under control of $P_{AMO,}$ hygromycin resistance cassette, amp^R	26
pHipZ7 eGFP	Contains gene encoding eGF-SKL under control of the P_{TEF1}, zeocine resitance cassette, amp^R	26

Table 3. List of primers used in this study.

Primers	Sequence
Cat_P_F	TTGGAAGCTTTATTGGTCTCGAGCCTTTGG
OL_CGF_F	TGGCTAATCACTGTTGAACAAAATGTCCAAGGGTGAAGAGC
OL_CGF_R	GCTCTTCACCCTTGGACATTTTGTTCAACAGTGATTAGCCA
sfGFP_O_R	TTTTACGCGTTTAGGATCCCTTATAAAGCTCG
Pmp20Pr_F	TTTTGCGGCCGCGATGCACACAAAAGGCCGAT
PP20_OL_F	CGGAGCTCTCAGGTTGAATATGTCCAAGGGTGAAGAGC
PP20_OL_R	GCTCTTCACCCTTGGACATATTCAACCTGAGAGCTCCG
Lon_P_F	TTTTGCGGCCGCAGGCCACGTTGGCTCTCA
Lon_OL_F	CCTTCAGTCAGATATATTCCACTAGCATGTCCAAGGGTGAAGAGC
Lon_OL_R	GCTCTTCACCCTTGGACATGCTAGTGGAATATATCTGACTGAAGG
sfGFP_SalI_R	TTCAGTCGACTTAGGATCCCTTATAAAGCTCG
Pcat_sel_F	CATGACCGAGTTTTTGTCCA
sfGFP_R	GTTGGCCAAGGAACAGGTAA
Ppmp20_sel_F	ACTCTGATCCCTGCTCCTGA
sfGFP_R	GTTGGCCAAGGAACAGGTAA
sfGFP_XhoI_R	TTCACTCGAGTTAGGATCCCTTATAAAGCTCG
C8BNF3_FP	GGGGACAAGTTTGTACAAAAAAGCAGGCTTTT TTTCCAGACAATTGCTGAGATTC

Table 3. (continued)

Primers	Sequence
C8BNF3_RP	GGGGACCACTTTGTACAAGAAAGCTGGGTGTT AGAGCTTGGTGAATCTAAGGTATG
C8BNF4_FP	GGGGACAAGTTTGTACAAAAAAGCAGGCTTT ATAAAAATCCACGGTTCAAAAA
C8BNF4_RP	GGGGACCACTTTGTACAAGAAAGCTGGGTGC TACAGATGCTCCAAAACAGC
P_{AMO}–FP	CTCTGACTTGAGCGTCGATT
GFP_RP	AAGTCGTGCTGCTTCATGTG
F3_HindIII_FP	CCCAAGCTTGGACAACAAGCCATTCTCCT
F3_BglII_RP	GGAAGATCTGAGCTTGGTGAATCTAAGGT
F3_cPCR_FP	GAAATTGCCAACTACTGAGC
mGFP_RP	ACTTGTACAGCTCGTCCATG
F4_NruI_FP	GGGTCGCGAAAAGACATATTCCAGCGTTT
F4_BglII_RP	GGAAGATCTCAGATGCTCCAAAACAGCTT
F4_cPCR_FP	TCAGACATATGGGGGTGATG
HpC8BNF3_Del_F	TGACTTCACCCCTGTGTGCACTACCGAGTTGGGTGC ATTTGCCAAATTGACCCACACACCATAGCTTCAAAA
HpC8BNF3_Del_R	AAGCAGGATAAGTCATGATCAGTCTAACTTTCTTAG CAGGATCGATGATGAATCGACAAAGGAAAAGGGG
HpC8BNF4_Del_F	GACATTGGTGATTGTGGCTGCTCCGGGCGCATTCAC TCCAACCTGTACCGCCCACACACCATAGCTTCAAAA
HpC8BNF4_Del_R	TTGGAGTTGCCCAAGGCCTTACCCCAAGCCGACTG GACGAATGGATCATTGCGTTTTCGACACTGGATGG
HpF3cPCR_F	AACAGATCTACAGGTCCGCTATAAT
Zeo_R	GAAGTGCACGCAGTTGCC
HpF4cPCR_F	TTGGCGTGAACCAGAAACT
Hyg_R	CAATGACCGCTGTTATGCG

Construction of reporter strains

The *CAT*, *PMP20* and *PLN* promoter regions were amplified using primers Cat_P_F and OL_CGF_R , Pmp20Pr_F and PP20_OL_R and Lon_P_F and Lon_OL_R. The sfGFP ORF was amplified using OL_CGF_F and sfGFP_O_R, PP20_OL_F and sfGFP_XhoI_R and Lon_OL_F and sfGFP_SalI_R primer combinations and the pMaM17 plasmid as a template. Overlap PCR was performed using amplicons obtained from the above mentioned three PCR reactions for construction of the PCAT_sfGFP (1569 bp), PPMP20_sfGFP (1437 bp) and PPLN_sfGFP (1743 bp) fusion products. Subsequently, the pHIPZ_mGFP fusinator plasmid was used for inserting PCAT_sfGFP and pHIPZ7_eGFP fusinator for PPMP20_sfGFP and PPLN_sfGFP. The amplicons and vector were digested using *Hin*dIII, *Mlu*I and *Not*I, *Xho*I and NotI, SalI enzyme combinations and ligated to obtain pHIPZ9_sfGFP, pHIPZ_PPMP20_sfGFP and pHIPZ_PPLN_sfGFP plasmid. These plasmids were linearized with *Psy*I and *Bpu*1102l respectively, prior to transformation into *H. polymorpha* WT cells. The transformants were

checked by colony PCR using primers Pcat_sel_F, sfGFP_R and PPmp20_sel_F, sfGFP_R and Plon_sel_F, sfGFP_R.

Construction of strains producing GFP_C8BNF3 and GFP_C8BNF4

Constructs encoding fusion proteins containing GFP at the N-terminus of *C8BNF3* and *C8BNF4*, under the control of the amine oxidase promoter (P_{AMO}) were obtained using Gateway Technology (Invitrogen) as described in Gateway manual (Magnani et al., 2006). Entry plasmids pENTR P_{AMO}GFP and pENTR T_{AMO} (Bener Aksam et al., 2008)as well as pENTR C8BNF3 and pENTR C8BNF4, which were constructed by PCR based methods, were used. Primers C8BNF3_F/ C8BNF3_RP and C8BNF4_FP/C8BNF4_RP were used to amplify *C8BNF3* and *C8BNF4*, respectively, after the start codon (ATG) using genomic DNA as a template. The constructs were cloned into pDONR221 plasmids by the Gateway BP reaction. Positive clones were selected and checked by restriction digestion using enzymes *Ssp*I and *Mun*I for C8BNF3 and *Eco*RV for C8BNF4. The pENTR P_{AMO}GFP, pENTR T_{AMO}, pENTR C8BNF3 and pENTR C8BNF4 plasmids were recombined with pDEST R4R3 plasmid by the Gateway LR reaction to form pDEST P_{AMO}-GFP-C8BNF3-T_{AMO} and pDEST P_{AMO}-GFP-C8BNF4-T_{AMO} respectively. Positive clones were selected and checked by restriction enzymes *Ssp*I and *Mun*IS. The final destination plasmids were linearized using *Ade*I and transformed into the genome of the *H. polymorpha* DsRed-SKL strain. The transformants were checked by colony PCR using primers Pamo_FP and GFP_RP.

Construction of strains producing C-terminal GFP fusions of C8BNF3 and C8BNF4

The C terminal part of *C8BNF3* and *C8BNF4* were amplified using primers F3_HindIII_F, F3_BglII_R with overhangs of *Hin*dIII and *Bgl*II restriction sites and F4_NruI_F and F4_ BglII_R with overhangs of *Nru*I and *Bgl*II restriction sites respectively. The PCR products were digested using the corresponding enzymes and cloned into plasmid pHIPZ-mGFP fusinator. The plasmid was linearized using *Van91*l and *Eco91*I and transformed into *H. polymorpha* WT strain. Transformants were checked by cPCR using primers F3_cPCR_FP and mGFP_RP for C8BNF3 and F4_cPCR_FP and mGFP_RP for C8BNF4.

Construction of deletion strains Δ*c8bnf3* and Δ*c8bnf4*

C8BNF3 gene was deleted in the WT *H. polymorpha* Pmp47-GFP containing strain (25) by replacing the ORF with a zeocin resistance cassette from the pHIPZ_mGFP fusinator plasmid using primers HpC8BNF3_Del_F and HpC8BNF3_Del_R. *C8BNF4* gene was deleted in the same strain as well as in Δ*pmp20* [11] strain by replacing the ORF with a hygromycin B resistance cassette (HPH) from plasmid pSEM04 using primers HpC8BNF4_Del_F and HpC8BNF4_Del_R. The PCR products were transformed into WT *H. polymorpha* Pmp47-GFP strain. Transformants were selected on zeocin and hygromycin plates and checked by colony PCR using primers HpF3cPCR_F/ Zeo_R for Δ*c8bnf3* and HpF4cPCR_F/ Hyg_R for Δ*c8bnf4* and Δ*c8bnf4*Δ*pmp20*. Correct integration was confirmed by Southern blotting.

Construction of plasmids encoding His_6GST-C8BNF3 and His_6GST-C8BNF4

For the production of antibodies, *C8BNF3* and *C8BNF4* genes along with *Nco*I/*Hind*III and *Nco*I/*Sal*I restriction enzyme sites, were amplified using genomic DNA as a template and primer combinations HisF3 NcoI_F/HisF3 HindIII_R and HisF4 NcoI_F/HisF4 SalI_R, respectively. *Nco*I-*Hind*III and *Nco*I-*Sal*I digested PCR fragment were used for ligation with *Nco*I-*Hind*III and *Nco*I-*Sal*I digested pETM30 harbouring the GST-His 6 tag.

Cell fractionation and purification of peroxisomes

Cells were homogenized and an organellar pellet fraction was prepared as described previously [32,33]. For the separation of peroxisomes, a discontinuous gradient was used with sucrose concentrations (w/w) varying from 65% - 44%. After the addition of the organellar pellet and an overlay containing 35% sucrose, the gradient was centrifuged using a Sorvall SV 288 rotor at 18,000 rpm for 2.5 hours, 4 °C. Gradients were collected in 2 ml fractions.

For cytochrome c oxidase enzyme acitivity, the initial decrease in the absorbance at 550 nm was measured in duplo using 2 different sample volumes essentially as described before [34]. Protein concentrations were measured using Bradford assay [35].

Mass spectrometric analysis

Peroxisomal peak fractions from gradients of organelle pellets obtained from control and cells exposed to stress were loaded onto an SDS PAGE gel followed by coomassie brilliant blue staining. Protein bands were excised from the gel, washed with a solution containing 100 mM ammonium bicarbonate in 100% acetonitrile and suspended in a solution containing 100 mM ammonium bicarbonate. Proteolytic treatment was performed using 10 ng/µl Trypsin (Promega) in 100 mM ammonium bicarbonate at 37°C, overnight. The peptides were extracted with 75% acetonitrile and 25% formic acid in water and analyzed by nano liquid chromatography-tandem mass spectrometry (nLC-MS/MS) [36]. Mass spectrometry (MS) data were analyzed with PEAKS 7.0 software (Bioinformatics Solutions Inc).

The pie-chart summarizing subcellular distribution of the putative *S. cerevisia*e homologues of the identified *H. polymorpha* proteins was prepared based on the SGD-yeast GFP fusion localization database.

Multiple sequence alignments of protein sequences were generated using ClustalW2 (http://www.ebi.ac.uk/Tools/msa/clustalw2/) and visualized with GeneDoc (http://www.nrbsc.org/old/gfx/genedoc/).

Protein purification and preparation of antibodies

H. polymorpha C8BNF3 and C8BNF4 with a cleavable His6-GST tag were produced in *E. coli* BL21 (DE3) RIL. Cells were grown at 37°C to an OD_{600} of 0.6 in Terrific Broth (TB) medium, transferred to 21°C and grown until an OD_{600} of 1.5. Gene expression was induced with 0.05mM IPTG (Invitrogen) for 16 h and cells were harvested by centrifugation. Cell pellets were resuspended in lysis buffer (50mM Tris-HCl pH 7.5, 150mM NaCl, 1% glycerol, 1mM DTT, 1mg/ml lysozyme, 10µg/ml DNase) and passed two times through a French press. Cell

debris was removed by centrifugation and lysates were loaded onto glutathione sepharose-4B resin (GE Healthcare) pre-equilibrated with lysis buffer. The resin was extensively washed with lysis buffer and His6-GST tagged proteins were eluted using lysis buffer containing 20mM reduced glutathione. The GST tag was cleaved from the protein using TEV protease and samples were passed through a Ni-NTA column. The peak fractions were subjected to gel filtration using a Superdex 200 (16/60) column (GE Healthcare) equilibrated with 25mM Tris, 150mM NaCl, 1mM 2-mercaptoethanol, pH 7.5. The presence of purified C8BNF3 and C8BNF4 was confirmed using SDS-PAGE and coomassie brilliant blue staining. The purified proteins were used for antibody generation in rabbit (Eurogentec).

Biochemical techniques

Extracts made from yeast cells treated with 12.5% trichloroacetic acid (TCA) were prepared for SDS-PAGE and Western blotting (WB) as detailed previously [37]. Equal amounts of proteins were loaded per lane. Blots were probed with rabbit polyclonal antisera against C8BNF3, C8BNF4 or elongation factor-1α (Ef1α).

Flow cytometry

Fluorescence-activated cell sorter (FACS) analysis was performed with a FACS Aria II Cell sorter (BD Biosciences). Cells were diluted using water after one hour of stress treatment and the fluorescence signal of individual cells was captured for 10,000 events at a speed of 500-1000 events per second. GFP fluorescence was measured using a 488 nm laser, 505 nm long pass mirror and 520/50nm band-pass filter. FACSDiva software version 6.1.2 was used for data acquisition and analysis. The presented data represents mean fluorescence intensity of the cells in different stress conditions treated in the same way.

Fluorescence microscopy

All images were made at room temperature using a 100x 1.30 NA Plan Neofluar objective. Wide-field images were made using a Zeiss Axioscope A1 fluorescence microscope (Carl Zeiss, Sliedrecht, The Netherlands). Images were taken using a Coolsnap HQ2 digital camera and Micro Manager software. A 470/40 nm bandpass excitation filter, a 495 nm dichromatic mirror and a 525/50 nm bandpass emission filter was used to visualize the GFP signal. DsRed fluorescence was visualized with a 546/12 nm bandpass excitation filter, a 560 nm dichromatic mirror and a 575/640 nm bandpass emission filter.

Electron microscopy

Cells were fixed in a mixture of 0.2% glutaraldehyde and 3% formaldehyde in 0.1M cacodylate buffer pH 7.2 for 4h on ice. Cells were embedded in Unicryl (Aurion, 14660). Unicryl was polymerized for 4 days under UV light at 10 °C. Immuno-gold labeling was performed on 70 nm ultrathin sections using antisera against C8BNF3 followed by gold conjugated goat anti-rabbit antiserum (Aurion, 806.011). Sections were post-stained with a mixture of 0.5% uranyl acetate and 0.2% methylcellulose before viewing them in a Philips CM12 electron microscope.

Acknowledgements

We thank Bohdan Lewków (Master student) for antibody production.

References

1. Smith JJ & Aitchison JD (2013) Peroxisomes take shape. *Nat. Rev. Mol. Cell Biol.* **14**, 803–817.
2. van der Klei IJ & Veenhuis M (2013) The versatility of peroxisome function in filamentous fungi. *Subcell. Biochem.* **69**, 135–152.
3. Dixit E, Boulant S, Zhang Y, Lee ASY, Odendall C, Shum B, Hacohen N, Chen ZJ, Whelan SP, Fransen M, Nibert ML, Superti-Furga G & Kagan JC (2010) Peroxisomes Are Signaling Platforms for Antiviral Innate Immunity. *Cell* **141**, 668–681.
4. Lazarow PB (2011) Viruses exploiting peroxisomes. *Curr. Opin. Microbiol.* **14**, 458–469.
5. Antonenkov VD, Grunau S, Ohlmeier S & Hiltunen JK (2009) Peroxisomes Are Oxidative Organelles. *Antioxid. Redox Signal.* **13**, 525–537.
6. Ma C, Hagstrom D, Polley SG & Subramani S (2013) Redox-regulated Cargo Binding and Release by the Peroxisomal Targeting Signal Receptor, Pex5. *J. Biol. Chem.* **288**, 27220–27231.
7. Ohdate T & Inoue Y (2012) Involvement of glutathione peroxidase 1 in growth and peroxisome formation in Saccharomyces cerevisiae in oleic acid medium. *Biochim. Biophys. Acta BBA - Mol. Cell Biol. Lipids* **1821**, 1295–1305.
8. Río D, A L & López-Huertas E (2016) ROS Generation in Peroxisomes and its Role in Cell Signaling. *Plant Cell Physiol.* **57**, 1364–1376.
9. Van Dijken JP, Veenhuis M, Vermeulen CA & Harder W (1975) Cytochemical localization of catalase activity in methanol-grown Hansenula polymorpha. *Arch. Microbiol.* **105**, 261–267.
10. Aksam EB, Koek A, Kiel JAKW, Jourdan S, Veenhuis M & van der Klei IJ (2007) A peroxisomal lon protease and peroxisome degradation by autophagy play key roles in vitality of Hansenula polymorpha cells. *Autophagy* **3**, 96–105.
11. Bener Aksam E, Jungwirth H, Kohlwein SD, Ring J, Madeo F, Veenhuis M & van der Klei IJ (2008) Absence of the peroxiredoxin Pmp20 causes peroxisomal protein leakage and necrotic cell death. *Free Radic. Biol. Med.* **45**, 1115–1124.
12. Söding J, Biegert A & Lupas AN (2005) The HHpred interactive server for protein homology detection and structure prediction. *Nucleic Acids Res.* **33**, W244-248.
13. Quevillon E, Silventoinen V, Pillai S, Harte N, Mulder N, Apweiler R & Lopez R (2005) InterProScan: protein domains identifier. *Nucleic Acids Res.* **33**, W116-120.
14. Navarro-Tapia E, Nana RK, Querol A & Pérez-Torrado R (2016) Ethanol Cellular Defense Induce Unfolded Protein Response in Yeast. *Front. Microbiol.* **7**.
15. Ryabova OB, Chmil OM & Sibirny AA (2003) Xylose and cellobiose fermentation to ethanol by the thermotolerant methylotrophic yeast Hansenula polymorpha. *FEMS Yeast Res.* **4**, 157–164.
16. Park SG, Cha M-K, Jeong W & Kim I-H (2000) Distinct Physiological Functions of Thiol Peroxidase Isoenzymes in Saccharomyces cerevisiae. *J. Biol. Chem.* **275**, 5723–5732.
17. Pedrajas JR, Miranda-Vizuete A, Javanmardy N, Gustafsson J-Å & Spyrou G (2000) Mitochondria of Saccharomyces cerevisiae Contain One-conserved Cysteine Type Peroxiredoxin with Thioredoxin Peroxidase Activity. *J. Biol. Chem.* **275**, 16296–16301.
18. Akiba S, Dodia C, Chen X & Fisher AB (1998) Characterization of acidic Ca(2+)-independent phospholipase A2 of bovine lung. *Comp. Biochem. Physiol. B Biochem. Mol. Biol.* **120**, 393–404.
19. Fisher AB & Dodia C (1996) Role of phospholipase A2 enzymes in degradation of dipalmitoylphosphatidylcholine by granular pneumocytes. *J. Lipid Res.* **37**, 1057–1064.
20. Kang SW, Baines IC & Rhee SG (1998) Characterization of a Mammalian Peroxiredoxin That Contains One Conserved Cysteine. *J. Biol. Chem.* **273**, 6303–6311.
21. Claros MG & Vincens P (1996) Computational method to predict mitochondrially imported proteins and their targeting sequences. *Eur. J. Biochem.* **241**, 779–786.

22. Banmeyer I, Marchand C, Verhaeghe C, Vucic B, Rees J-F & Knoops B (2004) Overexpression of human peroxiredoxin 5 in subcellular compartments of Chinese hamster ovary cells: effects on cytotoxicity and DNA damage caused by peroxides. *Free Radic. Biol. Med.* **36**, 65–77.
23. Kropotov A, Usmanova N, Serikov V, Zhivotovsky B & Tomilin N (2007) Mitochondrial targeting of human peroxiredoxin V protein and regulation of PRDX5 gene expression by nuclear transcription factors controlling biogenesis of mitochondria. *FEBS J.* **274**, 5804–5814.
24. Singh AK, Dhaunsi GS, Gupta MP, Orak JK, Asayama K & Singh I (1994) Demonstration of glutathione peroxidase in rat liver peroxisomes and its intraorganellar distribution. *Arch. Biochem. Biophys.* **315**, 331–338.
25. Wong C-M, Siu K-L & Jin D-Y (2004) Peroxiredoxin-null Yeast Cells Are Hypersensitive to Oxidative Stress and Are Genomically Unstable. *J. Biol. Chem.* **279**, 23207–23213.
26. van Dijken JP, Otto R & Harder W (1976) Growth of Hansenula polymorpha in a methanol-limited chemostat. Physiological responses due to the involvement of methanol oxidase as a key enzyme in methanol metabolism. *Arch. Microbiol.* **111**, 137–144.
27. Fernandes L, Rodrigues-Pousada C & Struhl K (1997) Yap, a novel family of eight bZIP proteins in Saccharomyces cerevisiae with distinct biological functions. *Mol. Cell. Biol.* **17**, 6982–6993.
28. Gasch AP, Spellman PT, Kao CM, Carmel-Harel O, Eisen MB, Storz G, Botstein D & Brown PO (2000) Genomic expression programs in the response of yeast cells to environmental changes. *Mol. Biol. Cell* **11**, 4241–4257.
29. Kwolek-Mirek M, Bednarska S, Bartosz G & Biliński T (2009) Acrolein toxicity involves oxidative stress caused by glutathione depletion in the yeast Saccharomyces cerevisiae. *Cell Biol. Toxicol.* **25**, 363–378.
30. Lee J, Spector D, Godon C, Labarre J & Toledano MB (1999) A New Antioxidant with Alkyl Hydroperoxide Defense Properties in Yeast. *J. Biol. Chem.* **274**, 4537–4544.
31. Faber KN, Haima P, Harder W, Veenhuis M & Ab G (1994) Highly-efficient electrotransformation of the yeast Hansenula polymorpha. *Curr. Genet.* **25**, 305–310.
32. Baerends RJ, Rasmussen SW, Hilbrands RE, van der Heide M, Faber KN, Reuvekamp PT, Kiel JA, Cregg JM, van der Klei IJ & Veenhuis M (1996) The Hansenula polymorpha PER9 gene encodes a peroxisomal membrane protein essential for peroxisome assembly and integrity. *J. Biol. Chem.* **271**, 8887–8894.
33. Knoops K, Manivannan S, Cepinska MN, Krikken AM, Kram AM, Veenhuis M & van der Klei IJ (2014) Preperoxisomal vesicles can form in the absence of Pex3. *J. Cell Biol.* **204**, 659–668.
34. Douma AC, Veenhuis M, Koning W de, Evers M & Harder W (1985) Dihydroxyacetone synthase is localized in the peroxisomal matrix of methanol-grown <Emphasis Type=”Italic”>Hansenula polymorpha</Emphasis>. *Arch. Microbiol.* **143**, 237–243.
35. Bradford MM (1976) A rapid and sensitive method for the quantitation of microgram quantities of protein utilizing the principle of protein-dye binding. *Anal. Biochem.* **72**, 248–254.
36. Dashty M, Motazacker MM, Levels J, de Vries M, Mahmoudi M, Peppelenbosch MP & Rezaee F (2014) Proteome of human plasma very low-density lipoprotein and low-density lipoprotein exhibits a link with coagulation and lipid metabolism. *Thromb. Haemost.* **111**, 518–530.
37. Baerends RJ, Faber KN, Kram AM, Kiel JA, van der Klei IJ & Veenhuis M (2000) A stretch of positively charged amino acids at the N terminus of Hansenula polymorpha Pex3p is involved in incorporation of the protein into the peroxisomal membrane. *J. Biol. Chem.* **275**, 9986–9995.
38. Ledeboer AM, Edens L, Maat J, Visser C, Bos JW, Verrips CT, Janowicz Z, Eckart M, Roggenkamp R & Hollenberg CP (1985) Molecular cloning and characterization of a gene coding for methanol oxidase in Hansenula polymorpha. *Nucleic Acids Res.* **13**, 3063–3082.
39. Didion T & Roggenkamp R (1992) Targeting signal of the peroxisomal catalase in the methylotrophic yeast Hansenula polymorpha. *FEBS Lett.* **303**, 113–116.
40. Kiel JAKW, Titorenko VI, Van Der Klei IJ & Veenhuis M (2007) Overproduction of translation elongation factor 1-α (eEF1A) suppresses the peroxisome biogenesis defect in a Hansenula polymorpha pex3 mutant via translational read-through. *FEMS Yeast Res.* **7**, 1114–1125.

41. Krikken AM, Veenhuis M & van der Klei IJ (2009) Hansenula polymorpha pex11 cells are affected in peroxisome retention. *FEBS J.* **276**, 1429–1439.
42. Suwannarangsee S, Oh D-B, Seo J-W, Kim CH, Rhee SK, Kang HA, Chulalaksananukul W & Kwon O (2010) Characterization of alcohol dehydrogenase 1 of the thermotolerant methylotrophic yeast Hansenula polymorpha. *Appl. Microbiol. Biotechnol.* **88**, 497–507.
43. Ozimek P, van Dijk R, Latchev K, Gancedo C, Wang DY, van der Klei IJ & Veenhuis M (2003) Pyruvate Carboxylase Is an Essential Protein in the Assembly of Yeast Peroxisomal Oligomeric Alcohol Oxidase. *Mol. Biol. Cell* **14**, 786–797.
44. Laht S, Karp H, Kotka P, Järviste A & Alamäe T (2002) Cloning and characterization of glucokinase from a methylotrophic yeast Hansenula polymorpha: different effects on glucose repression in H. polymorpha and Saccharomyces cerevisiae. *Gene* **296**, 195–203.
45. Agaphonov MO, Packeiser AN, Chechenova MB, Choi E-S & Ter-Avanesyan MD (2001) Mutation of the homologue of GDP-mannose pyrophosphorylase alters cell wall structure, protein glycosylation and secretion in Hansenula polymorpha. *Yeast* **18**, 391–402.
46. Titorenko VI, Evers ME, Diesel A, Samyn B, van Beeumen J, Roggenkamp R, Kiel JAKW, van der Klei IJ & Veenhuis M (1996) Identification and characterization of cytosolic Hansenula polymorpha proteins belonging to the Hsp70 protein family. *Yeast* **12**, 849–857.
47. Klei IJ van der, Heide M van der, Baerends RJS, Rechinger K-B, Nicolay K, Kiel J a. KW & Veenhuis M (1998) The Hansenula polymorpha per6 mutant is affected in two adjacent genes which encode dihydroxyacetone kinase and a novel protein, Pak1p, involved in peroxisome integrity. *Curr. Genet.* **34**, 1–11.
48. Cox H, Mead D, Sudbery P, Eland RM, Mannazzu I & Evans L (2000) Constitutive expression of recombinant proteins in the methylotrophic yeast Hansenula polymorpha using the PMA1 promoter. *Yeast* **16**, 1191–1203.
49. Bae J-H, Sohn J-H, Rhee S-K & Choi E-S (2005) Cloning and characterization of the Hansenula polymorpha PEP4 gene encoding proteinase A. *Yeast* **22**, 13–19.
50. Bellu AR, van der Klei IJ, Rechinger KB, Yavuz M, Veenhuis M & Kiel J a. KW (1999) Characterization of the Hansenula polymorpha CPY gene encoding carboxypeptidase Y. *Yeast* **15**, 181–189.
51. Biswas D, Datt M, Ganesan K & Mondal AK (2010) Cloning and characterization of thermotolerant xylitol dehydrogenases from yeast <Emphasis Type="Italic">Pichia angusta</Emphasis>. *Appl. Microbiol. Biotechnol.* **88**, 1311–1320.
52. Nagotu S, Saraya R, Otzen M, Veenhuis M & van der Klei IJ (2008) Peroxisome proliferation in Hansenula polymorpha requires Dnm1p which mediates fission but not de novo formation. *Biochim. Biophys. Acta BBA - Mol. Cell Res.* **1783**, 760–769.
53. Stasyk OV, Stasyk OG, Komduur J, Veenhuis M, Cregg JM & Sibirny AA (2004) A Hexose Transporter Homologue Controls Glucose Repression in the Methylotrophic Yeast Hansenula polymorpha. *J. Biol. Chem.* **279**, 8116–8125.
54. Otzen M, Krikken AM, Ozimek PZ, Kurbatova E, Nagotu S, Veenhuis M, Klei VD & J I (2006) In the yeast Hansenula polymorpha, peroxisome formation from the ER is independent of Pex19p, but involves the function of p24 proteins. *FEMS Yeast Res.* **6**, 1157–1166.
55. Butler G, Kenny C, Fagan A, Kurischko C, Gaillardin C & Wolfe KH (2004) Evolution of the MAT locus and its Ho endonuclease in yeast species. *Proc. Natl. Acad. Sci. U. S. A.* **101**, 1632–1637.
56. Klabunde J, Kleebank S, Piontek M, Hollenberg CP, Hellwig S & Degelmann A (2007) Increase of calnexin gene dosage boosts the secretion of heterologous proteins by Hansenula polymorpha. *Fems Yeast Res.* **7**, 1168–1180.
57. Gidijala L, Klei VD, J I, Veenhuis M & Kiel JAKW (2007) Reprogramming Hansenula polymorpha for penicillin production: expression of the Penicillium chrysogenum pcl gene. *FEMS Yeast Res.* **7**, 1160–1167.
58. Chechenova MB, Romanova NV, Deev AV, Packeiser AN, Smirnov VN, Agaphonov MO & Ter-Avanesyan MD (2004) C-Terminal Truncation of α-COP Affects Functioning of Secretory Organelles and Calcium Homeostasis in Hansenula polymorpha. *Eukaryot. Cell* **3**, 52–60.

59. Reinders A, Romano I, Wiemken A & De Virgilio C (1999) The Thermophilic Yeast Hansenula polymorpha Does Not Require Trehalose Synthesis for Growth at High Temperatures but Does for Normal Acquisition of Thermotolerance. *J. Bacteriol.* **181**, 4665–4668.
60. Fry MR, Thomson JM, Tomasini AJ & Jr WAD (2006) Role of Vac8 in Cellular Degradation Pathways in Pichia pastoris. *Autophagy* **2**, 280–288.
61. Kiel JAKW, Veenhuis M & van der Klei IJ (2006) PEX Genes in Fungal Genomes: Common, Rare or Redundant. *Traffic* **7**, 1291–1303.
62. Kiel J a. KW, Hilbrands RE, van der Klei IJ, Rasmussen SW, Salomons FA, van der Heide M, Faber KN, Cregg JM & Veenhuis M (1999) Hansenula polymorpha Pex1p and Pex6p are peroxisome-associated AAA proteins that functionally and physically interact. *Yeast* **15**, 1059–1078.
63. Woong Kim M, Agaphonov MO, Kim J-Y, Ki Rhee S & Ah Kang H (2002) Sequencing and functional analysis of the Hansenula polymorpha genomic fragment containing the YPT1 and PMI40 genes. *Yeast* **19**, 863–871.
64. Serrani F & Berardi E (2005) The NII2 gene of Hansenula polymorpha is involved in nitrite assimilation. *FEMS Yeast Res.* **5**, 999–1007.
65. Baker RE & Rogers K (2006) Phylogenetic Analysis of Fungal Centromere H3 Proteins. *Genetics* **174**, 1481–1492.
66. Meijer WH, van der Klei IJ, Veenhuis M & Kiel JAKW (2007) ATG genes involved in non-selective autophagy are conserved from yeast to man, but the selective Cvt and pexophagy pathways also require organism-specific genes. *Autophagy* **3**, 106–116.
67. Koek A, Komori M, Veenhuis M & Van Der Klei IJ (2007) A comparative study of peroxisomal structures in Hansenula polymorpha pex mutants. *FEMS Yeast Res.* **7**, 1126–1133.
68. Saraya R, Cepińska MN, Kiel JAKW, Veenhuis M & der Klei IJ van (2010) A conserved function for Inp2 in peroxisome inheritance. *Biochim. Biophys. Acta BBA - Mol. Cell Res.* **1803**, 617–622.
69. Yamada K & Tani Y (1987) Diversity of Glycerol Dehydrogenase in Methylotrophic Yeasts. *Agric. Biol. Chem.* **51**, 2401–2407.
70. Bruinenberg PG, Evers M, Waterham HR, Kuipers J, Arnberg AC & Ab G (1989) Cloning and sequencing of the peroxisomal amine oxidase gene from Hansenula polymorpha. *Biochim. Biophys. Acta BBA - Gene Struct. Expr.* **1008**, 157–167.
71. Monastyrska I, Van Der Heide M, Krikken AM, Kiel JAKW, Van Der Klei IJ & Veenhuis M (2005) Atg8 is Essential for Macropexophagy in Hansenula polymorpha. *Traffic* **6**, 66–74.
72. van der Heide M, Hollenberg CP, van der Klei IJ & Veenhuis M (2002) Overproduction of BiP negatively affects the secretion of Aspergillus niger glucose oxidase by the yeast Hansenula polymorpha. *Appl. Microbiol. Biotechnol.* **58**, 487–494.
73. Sangwallek J, Kaneko Y, Tsukamoto T, Marui M, Sugiyama M, Ono H, Bamba T, Fukusaki E & Harashima S (2014) Cloning and functional analysis of HpFAD2 and HpFAD3 genes encoding Δ12- and Δ15-fatty acid desaturases in Hansenula polymorpha. *Gene* **533**, 110–118.
74. Agaphonov MO, Plotnikova TA, Fokina AV, Romanova NV, Packeiser AN, Kang HA & Ter-Avanesyan MD (2007) Inactivation of the Hansenula polymorpha PMR1 gene affects cell viability and functioning of the secretory pathway. *FEMS Yeast Res.* **7**, 1145–1152.
75. Kim S-Y, Sohn J-H, Ah Kang H, Yoo S-K, Pyun Y-R & Choi E-S (2001) Cloning and characterization of the Hansenula polymorpha homologue of the Saccharomyces cerevisiae MNN9 gene. *Yeast* **18**, 455–461.
76. Ozimek P, Lahtchev K, Kiel JAKW, Veenhuis M & van der Klei IJ (2004) Hansenula polymorpha Swi1p and Snf2p are essential for methanol utilisation. *FEMS Yeast Res.* **4**, 673–682.
77. Prasitchoke P, Kaneko Y, Bamba T, Fukusaki E, Kobayashi A & Harashima S (2007) Identification and characterization of a very long-chain fatty acid elongase gene in the methylotrophic yeast, Hansenula polymorpha. *Gene* **391**, 16–25.
78. Haan GJ, Faber KN, Baerends RJS, Koek A, Krikken A, Kiel JAKW, Klei IJ van der & Veenhuis M (2002) Hansenula polymorpha Pex3p Is a Peripheral Component of the Peroxisomal Membrane. *J. Biol. Chem.* **277**, 26609–26617.

79. Agaphonov MO, Sokolov SS, Romanova NV, Sohn J-H, Kim S-Y, Kalebina TS, Choi E-S & Ter-Avanesyan MD (2005) Mutation of the protein-O-mannosyltransferase enhances secretion of the human urokinase-type plasminogen activator in Hansenula polymorpha. *Yeast* **22**, 1037–1047.
80. Agaphonov MO, Poznyakovski AI, Bogdanova AI & Ter-Avanesyan MD (1994) Isolation and characterization of the LEU2 gene of Hansenula polymorpha. *Yeast Chichester Engl.* **10**, 509–513.
81. Kim MW, Kim EJ, Kim J-Y, Park J-S, Oh D-B, Shimma Y, Chiba Y, Jigami Y, Rhee SK & Kang HA (2006) Functional Characterization of the Hansenula polymorpha HOC1, OCH1, and OCR1 Genes as Members of the Yeast OCH1 Mannosyltransferase Family Involved in Protein Glycosylation. *J. Biol. Chem.* **281**, 6261–6272.
82. Song H, Qian W, Wang H & Qiu B (2010) Identification and functional characterization of the HpALG11 and the HpRFT1 genes involved in N-linked glycosylation in the methylotrophic yeast Hansenula polymorpha. *Glycobiology* **20**, 1665–1674.
83. Krappmann S, Pries R, Gellissen G, Hiller M & Braus GH (2000) HARO7 Encodes Chorismate Mutase of the Methylotrophic Yeast Hansenula polymorpha and Is Derepressed upon Methanol Utilization. *J. Bacteriol.* **182**, 4188–4197.
84. Stoyanov A, Petrova P, Lyutskanova D & Lahtchev K (2014) Structural and functional analysis of PUR2,5 gene encoding bifunctional enzyme of de novo purine biosynthesis in Ogataea (Hansenula) polymorpha CBS 4732T. *Microbiol. Res.* **169**, 378–387.
85. Merckelbach A, Gödecke S, Janowicz ZA & Hollenberg CP (1993) Cloning and sequencing of the ura3 locus of the methylotrophic yeast Hansenula polymorpha and its use for the generation of a deletion by gene replacement. *Appl. Microbiol. Biotechnol.* **40**, 361–364.
86. Esteban PF, Vazquez de Aldana CR & del Rey F (1999) Cloning and characterization of 1,3-beta-glucanase-encoding genes from non-conventional yeasts. *Yeast Chichester Engl.* **15**, 91–109.
87. Rodríguez C, Tejera P, Medina B, Guillén R, Domínguez Á, Ramos J & Siverio JM (2010) Ure2 Is Involved in Nitrogen Catabolite Repression and Salt Tolerance via Ca2+ Homeostasis and Calcineurin Activation in the Yeast Hansenula polymorpha. *J. Biol. Chem.* **285**, 37551–37560.
88. Phongdara A, Merckelbach A, Keup P, Gellissen G & Hollenberg CP (1998) Cloning and characterization of the gene encoding a repressible acid phosphatase (PHO1) from the methylotrophic yeast Hansenula polymorpha. *Appl. Microbiol. Biotechnol.* **50**, 77–84.
89. Haan GJ, van Dijk R, Kiel JAKW & Veenhuis M (2002) Characterization of the Hansenula polymorpha PUR7 gene and its use as selectable marker for targeted chromosomal integration. *FEMS Yeast Res.* **2**, 17–24.
90. Kato N, Omori Y, Tani Y & Ogata K (1976) Alcohol oxidases of Kloeckera sp. and Hansenula polymorpha. Catalytic properties and subunit structures. *Eur. J. Biochem.* **64**, 341–350.
91. Dhaunsi GS, Gulati S, Singh AK, Orak JK, Asayama K & Singh I (1992) Demonstration of Cu-Zn superoxide dismutase in rat liver peroxisomes. Biochemical and immunochemical evidence. *J. Biol. Chem.* **267**, 6870–6873.

Supplementary data

Table S1. Proteins identified by mass spectrometry in peroxisomal fractions from controls and cells exposed to ethanol stress.

S. No.	Name of the protein	Control	Ethanol stress	Reference	Localization
1	Alcohol oxidase	+	+	[38]	Peroxisome
2	Dihydroxyacetone synthase	+	+	[34]	Peroxisome
3	Catalase	+	+	[39]	Peroxisome
4	Aldehyde dehydrogenase	+	+		Cytosol
5	Formate dehydrogenase	+	+		Cytosol
6	Formaldehyde dehydrogenase	+	+	(Baerends *et al.*, 2002)	Cytosol
7	Elongation factor 1 alpha	+	+	[40]	Cytosol
8	**Peroxisome membrane protein 20 (Pmp20)**	**+**	**+**	**[11]**	**Peroxisome**
9	Pex11	+	+	[41]	Peroxisome
10	Alcohol dehydrogenase 1	+	+	[42]	Cytosol
11	Pyruvate carboxylase	+	+	[43]	Cytosol
12	Glucokinase	+	+	[44]	Cytosol
13	Mannose 1 phosphate guanyltransferase	+	+	[45]	Cytosol
14	Heat shock protein 70 2	+	-	[46]	Cytosol
15	**Putative peroxiredoxin (C8BNF3)**	**+**	**+**		
16	Dihydroxyacetone kinase	+	+	[47]	Peroxisome, Cytosol
17	Lon protease homolog 2	+	+	[10]	Peroxisome
18	DNA directed RNA polymerase	+	+		
19	Plasma membrane H+ATPase	+	+	[48]	Plasma membrane
20	**Putative peroxiredoxin (C8BNF4)**	**+**	**+**		
21	Proteinase A	+	+	[49]	Vacuole
22	Carboxypeptidase	+	+	[50]	Vacuole
23	Lon protease homolog	+	+		
24	Xylitol dehydrogenase	+	+	[51]	
25	**Putative peroxiredoxin (C8BNF0)**	**+**	**+**		
26	Heat Shock protein 70 1	+	+	[46]	Cytosol
27	Dynamin like GTP binding protein (Vps1)	+	-	[52]	Cytosol, Endosomes
28	DNA directed RNA polymerase	+	+		
29	Fatty acid synthetase beta subunit	+	+		
30	Hexose transporter-like GCR1	+	+	[53]	Cytosol, Nucleus
31	Fatty acid synthase alpha subunit	+	+		
32	Emp24	+	+	[54]	ER
33	Putative DIC1 protein	+	-	[55]	Mitochondria
34	Calnexin homologue	+	+	[56]	ER
35	**Putative peroxiredoxin (C8BNF2)**	**+**	**+**		
36	Putative cystathionine beta lyase, Met6	+	+	[57]	Cytosol
37	Alpha-COP-like protein,Opu27	+	+	[58]	Golgi
38	Alpha trehalose phosphate synthase, Tps1	+	-	[59]	
39	Vac8	+	+	[60]	Vacuole

Table S1. (continued)

S. No.	Name of the protein	Control	Ethanol stress	Reference	Localization
40	Pex10	+	+	[61]	Peroxisome
41	**Putative peroxiredoxin (C8BNE0)**	**+**	**+**		
42	Aminopeptidase	+	+		
43	Pex3	+	+	[61]	Peroxisome
44	Erp3	+	+	[54]	ER
45	Pex1	+	-	[62]	Peroxisome
46	GTP binding protein, Ypt1	+	+	[63]	ER, Golgi
47	Nii2	+	+	[64]	ER
48	Centromere H3 protein	+	+	[65]	Nucleus
49	Protein kinase TOR	+	-	[66]	Cytosol, Nucleus
50	Pex2	+	+	[67]	Peroxisome
51	Dynamin related protein	+	-	[52]	Mitochondria
52	Myo2	+	+	[68]	Cytosol, bud-neck
53	Glycerol dehydrogenase, Gdh1	+	+	[69]	Cytosol
54	Pex6	+	-	[62]	Peroxisome
55	Pex12	+	+	[67]	Peroxisome
56	Glycerol 3 phosphate dehydrogenase, Gpd1	+	+		
57	Peroxisomal primary amine oxidase, Amo	+	+	[70]	Peroxisome
58	Trehalose phosphate synthase subunit, Tps3	+	-		
59	Multifunctional tryptophan biosynthesis protein	+	-	[38]	Cytosol
60	Autophagy related protein 8, Atg8	+	-	[71]	Cytosol, vacuole
61	DNA-directed RNA polymerase	+	-		
62	78kDa glucose-regulated protein	+	-	[72]	ER
63	**Putative peroxiredoxin (C8BNF1)**	**+**	**+**		
64	Pex26	+	+	[61]	Peroxisome
65	Delta 12-fatty acid desaturase, FAD2	+	-	[73]	ER
66	Calcium transporting ATPase	+	-	[74]	Golgi
67	Mnn9	+	-	[75]	Golgi
68	Global transcription activator,Snf2	+	-	[76]	Nucleus
69	Elongation of fatty acid protein	+	-	[77]	ER
70	Pex8	+	-	[78]	Peroxisome
71	Dolichyl phosphate mannose protein	+	-	[79]	ER
72	Isopropylmalate dehydrogenase	+	-	[80]	Cytosol
73	Sugar transporter like protein	+	-		
74	Putative uncharacterized protein	+	-		
75	Orotate-phophoribosyltransferase	+	+		
76	Ocr1	+	-	[81]	Golgi
77	Autophagy related protein 27	+	-	[66]	
78	Putative uncharacterized protein	+	-		
79	Alpha 1 2-mannosyltransferase	+	-	[82]	ER
80	Frataxin	+	-		
81	Inositol 1 phosphate synthase	+	+		
82	Chorismate mutase	+	-	[83]	Cytosol, Nucleus

Table S1. (continued)

S. No.	Name of the protein	Control	Ethanol stress	Reference	Localization
83	Pur 2 5	+	-	[84]	Cytosol
84	Pex11	+	+	[61]	Peroxisome
85	Pex17	+	-	[61]	Peroxisome
86	Pex14	+	+	[61]	Peroxisome
87	Orotidine 5'phosphate decarboxylase, Ura3	+	+	[85]	Cytosol
88	Glucan 1 3-beta glucosidase	+	-	[86]	
89	Pex25	+	+	[61]	Peroxisome
90	Amm1	+	-		
91	Ure2	+	-	[87]	Cytosol
92	Repressible acid phosphatase	+	-	[88]	
93	Putative kinase Pak1	+	-	[47]	
94	Caspase	+	-	[11]	Cytosol, Nucleus
95	Pex22	+	+	[61]	Peroxisome
96	Phosphoribosylaminoimidazole – succinocarboxamide synthase,	+	-	[89]	Cytosol, Nucleus
97	Putative mannosyl transferase, Ocr5	+	-	[81]	ER, Golgi
98	Putative Sla 2 protein (actin associated protein-endocytosis)	+	-	[55]	
99	Cell wall protein Gas1	+	-		
100	Ubiquitin conjugating enzyme	-	+	[61]	
101	RNA Pol II second largest subunit	-	+		

* The order of the proteins is based on the % protein sequence coverage. Highlighted rows include the identified putative peroxiredoxins along with Pmp20. The mentioned localization is based on experimental data obtained for the *H. polymorpha* proteins..